JOURNAL OF AIRCRAFT
Vol. 47, No. 5, September–October 2010

Modeling of Pilot Landing Approach Control Using Stochastic Switched Linear Regression Model

Ryota Mori*
Electronic Navigation Research Institute, Tokyo 182-0012, Japan
and
Shinji Suzuki†
University of Tokyo, Tokyo 113-8656, Japan

DOI: 10.2514/1.C000204

Human pilot control during the landing approach is modeled using a stochastic switched model, which is a combination of the conventional linear regression model and a hidden Markov model. Using this model, the time histories of pilot control can be categorized in several states, such as pitch stabilizing mode. First, the selection of model inputs is discussed. Based on data obtained in flight simulator experiments, the pilot approach control model is constructed for several cases, with different wind conditions applying an expectation-maximization algorithm. The obtained models are analyzed with respect to the timing of state transitions and the stochastic-switched-model gain parameters. The current findings suggest that the proposed analysis method has a great potential to reveal a pilot's decision-making process.

I. Introduction

RECENT aircraft are equipped with an autolanding system, for which the performance is acceptable in most cases. While current autolanding systems can generate very precise control inputs, they cannot operate under critically severe wind conditions. Therefore, human pilot control is still important in emergencies when the autolanding system input is not reliable enough. Furthermore, even though human pilot control generally shows better landing performance, there is no sufficient understanding of the control strategy of human pilots yet. On the other hand, the human pilot can be a source of aircraft accidents. Over 70% of the fatal aviation accidents involved human factors, most related to poor judgment and decision making [1]. Thus, both auto pilot systems and human pilots have pros and cons, so the performance of autolanding systems can be improved if the advantages of man and machine can be put together. Therefore, it is important to reveal and understand thoroughly the human pilot control strategy.

Consequently, the authors aim at modeling human pilot control during the final landing phase to analyze the human pilot control. In the previous study, the flare maneuver was analyzed [2,3]. The flare maneuver is the lifting-the-nose control just before touchdown. This control is characterized by high nonlinearity, and it was modeled using a neural network [4]. A neural network and fuzzy systems are conventionally proposed to model nonlinear input/output relationships. In addition, a landing system based on a human skill model is suggested in a different manner [5]. However, these models are too complicated to evaluate the performance of the system and prove its stability. Therefore, a simple model is superior to a complicated one.

According to pilot comments, the landing control can be divided into two distinct phases: approach and flare, with the control strategy varying significantly between these phases. To make a successful landing, both the flare control and the approach control should be adequate. If these phases are modeled independently, the overall model can be simplified, which makes it easier to construct an autolanding system. Thus, in this paper, the first step to an approach model (i.e., longitudinal elevator control model) is constructed for human pilot control. During the approach control (usually above 100 or 200 ft altitude), a pilot has to follow the reference path (called a glide path) as well as adjust the proper airspeed and avoid a big attitude oscillation, using elevator and throttle controls under wind disturbance. The pilot obtains the necessary information from the instrument panel, which provides values of the pitch angle, the deviation angle from the glide path, airspeed, sink rate, altitude, and so on. The details are written in Sec. III.

To model the pilot's approach control, the stochastic switched linear regression model (SS model) is adopted. This model is composed of a conventional linear regression model with probabilistic change of several states using a hidden Markov model (HMM). The approach control is (relatively) easier than flare control and can be modeled more simply, which makes it easy to understand. Such an SS model has also been adopted to analyze human car-driving behavior and has showed a reasonably good performance [6].

This paper starts with a brief overview of the SS model, then a brief explanation of the acquisition of flight and control data during approach with a B747 simulator. Next, the human pilot approach model is constructed based on the SS model. Using this model, the pilot's reasoning at each state and the timing of switching states are discussed.

II. Overview of the Stochastic Switched Linear Regression Model

The SS model consists of a conventional linear regression model and a HMM. First, these models are explained, and then the parameter estimation technique is presented.

A. Linear Regression Model

The conventional linear regression model is used for system identification and is described by the following equation:

$$y_t = b_1 u_{1,t} + \cdots + b_n u_{n,t} + e_t \tag{1}$$

where, y_t and $u_{i,t}$ are the dependent variables (outputs) and the ith regressors (inputs) at time t, respectively. The regression coefficients are b_i to the ith input. An equation error with variance σ is e_t.

Received 1 December 2009; revision received 22 March 2010; accepted for publication 22 March 2010.

*Researcher, Air Traffic Management Department, 7-42-23 Jindaiji-Higashimachi, Chofu-shi.

†Professor, Department of Aeronautics and Astronautics, 7-3-1 Hongo, Bunkyo-ku. Senior Member AIAA.

Equation (1) can be simplified as follows:

$$y_t = \theta^T \psi_t + e_t; \qquad \theta = [\, b_1 \quad b_2 \quad \cdots \quad b_n \,]^T;$$
$$\psi_t = [\, u_{1,t} \quad u_{2,t} \quad \cdots \quad u_{n,t} \,]^T \tag{2}$$

Parameters θ are found by the least-squares fit of measurement data.

B. Hidden Markov Model

The HMM is a statistical model based on the standard Markov model and is a popular technique in the field of speech recognition [7]. This model can determine hidden parameters from observable data based on a probabilistic process. Figure 1 shows a simple ergodic HMM model.

C. Stochastic Switched Linear Regression Model

The SS model is a combination of the linear regression model and the HMM. Figure 2 shows the logic of a SS model. In this model, regression coefficients θ are predetermined for each state and switched in between, according to HMM state transition probabilities.

The output symbols and the output probabilities are defined as follows:

$$o_t = [\, y_t \quad \psi_t \,]; \qquad b_i(o_t) = \frac{1}{\sqrt{2\pi}\sigma_i} \exp\left(\frac{-e_{i,t}^2}{2\sigma_i^2}\right)$$

To construct a SS model, several parameters have to be set: 1) a_{ij}: the state transition probability, 2) π_i: the initial state probability, 3) θ_i: the regressor coefficients in each state, and 4) σ_i: the variance of equation error in each state.

These parameters can be estimated using an expectation-maximization algorithm, which uses supervised learning. Thus, the inputs and outputs to be used for the model should be prepared for learning. The parameter estimation process is described in detail in [6].

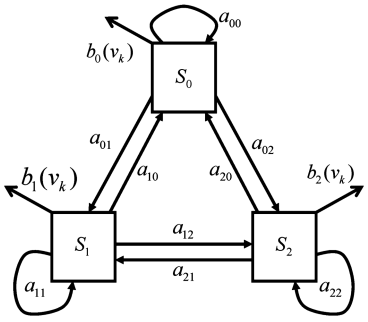

S_i : i^{th} discrete state
v_k : k^{th} output symbol (observable data)
a_{ij} : state transition probability from i^{th} state to j^{th} state
$b_i(v_k)$: output probability in i^{th} state at output symbol v_k

Fig. 1 Ergodic HMM model.

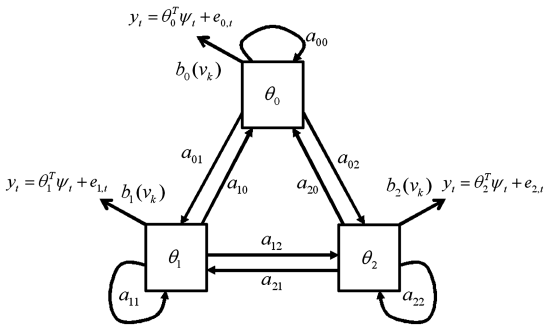

Fig. 2 Three states of SS model.

D. State Transition Process Identification by the Viterbi Algorithm

The HMM model switches between discrete states based on the state transition probability. An output symbol is generated according to the output probability of each state. Once this model is constructed, the most likely states in each time step can be obtained using Viterbi algorithm [7]. This algorithm does not assure the right sequences of states, but it shows the most likely state for each time step. It is calculated based on the following expressions:

$$\delta(i,t) = \max_j \{\delta(j,t-1) a_{ji} b_i(o_t)\};$$
$$\gamma(i,t) = \arg\max_j \{\delta(j,t-1) a_{ji} b_i(o_t)\}$$

where $\gamma(i,t)$ indicates the most likely state S_i at time t.

III. Construction of a Pilot Model for the Approach Phase

A. Approach Control Modeling

During the approach phase, the pilot relies on instrument panel and the out-the-window view (i.e., visual cues to obtain the information needed to execute adequate landing). The visual cues can give the pilot fast and reliable information, while the instrument panel has a slightly delayed response. However, if the aircraft is far from the airport, the visual cues have low sensitivity and the pilot cannot obtain sufficiently detailed information from them only. Therefore, during the approach phase (here, defined as the phase above 100 ft altitude), the instrument panel information is mainly used. According to pilot comments, the instrument panel provides sufficient information to control the elevator and throttle. Note that only longitudinal control is considered in this paper.

Figure 3 shows the relationship between the instrument panel and the aircraft states. As for longitudinal control, 1) the pitch angle, 2) the deviation angle from glide path, and 3) the airspeed are considered important for the pilot. It is assumed that the flight director system is not being used. The first white circle above the center line (optimal glide path) indicates a deviation of about 0.3 deg from the optimal glide path. Note that the glide path deviation is defined as an angle (i.e., the closer the aircraft is to the runway, the more sensitive the glide-path indication becomes). A pilot usually decreases the sensitivity to avoid instability. Although the proposed model does not explicitly include the sensitive effect, the timing of changing the states can be obtained. Therefore, it can be used as an indicator of the sensitivity to the glide-slope deviation. Based on pilot comments, during the approach phase, the target pitch angle is set in the pilot's mind (depending on the situation), and the elevator is controlled to maintain the target pitch angle. The situation is judged from the deviation angle from the glide path and airspeed.

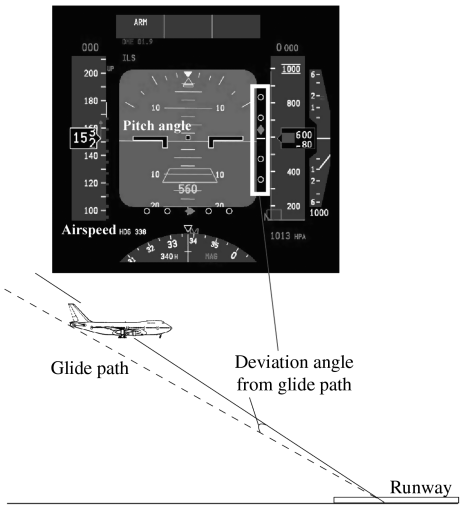

Fig. 3 Relationship between instrument panel and aircraft states.

Consequently, this approach control strategy is modeled with a SS model. Note that only elevator control is modeled in this paper. Within a state, it is assumed that the elevator is controlled only by pitch angle, and its derivative and the state is changed depending on the state transition probabilities. The inputs and the output of the model are defined as follows:

$$\psi_t = [\,\mathrm{Y}_{t=t-0.2} \quad \mathrm{dY/dt}_{t=t-0.2} \quad \mathrm{dY/dt}_{t=t-0.7} \quad 1.0];$$

$$y_t = \delta_{e\ t=t}$$

where Y is the pitch angle and δ_e is the elevator angle. According to pervious research [8], the input should include a 0.2 s time delay, which corresponds to the human response. Moreover, an extra, more delayed derivative of the pitch angle is included in the input. These three inputs can represent simple proportional-derivative (PD) control with time delay. The 4th input is a constant term, and can account for the trim adjustment.

B. Experiment Condition

To model the pilot's approach control, flight and pilot control data are necessary. Thus, a simulator experiment was carried out. The PC-based simulator is owned by the authors' laboratory as shown in Fig. 4, and models a B747 aircraft. The outside view is drawn by Microsoft Flight Simulator. The examinee was a retired B747 captain, who was asked to land the aircraft from 1000 ft altitude without any restrictions with four control devices (elevator, aileron, rudder, and throttle). The data was extracted between 100 and 1000 ft altitude and was used for training the SS-model parameters. The data sampling rate was 5 Hz. Two wind patterns were applied in the simulation: 1) turbulence, 2) 10 kt headwind with turbulence. Th e headwind decreases both the ground speed and the sink rate, which may affect the pilot control. Flight and control data were obtained 3 times for each wind condition.

Using the data, the pilot model was constructed for each case, i.e., six models in total were constructed. These are summarized in Table 1.

Table 1 Experiment Cases

Case	Wind
0–1	No constant wind and turbulence
0–2	No constant wind and turbulence
0–3	No constant wind and turbulence
10–1	10 kt headwind and turbulence
10–2	10 kt headwind and turbulence
10–3	10 kt headwind and turbulence

IV. Modeling Results

A. Detailed Analysis

First, one case (case 0-1) is chosen and analyzed in detail. Figure 5 shows the time histories of elevator angle, pitch angle, deviation angle from glide path, and throttle deflection.

If we look at the elevator angle, we see that the obtained model can imitate the pilot approach control with state transition. In this model, there are 4 state transitions, named a, b, c, and d. The states are categorized to three states; 1) standard state (which is defined as the most likely observable state), 2) stabilizing state, 3) path-fixing state, as will become clear from the results later. At state transition a, the aircraft deviates slightly from the glide path. From this point, the pitch angle and elevator angle oscillate with large magnitude. It seems that the pilot adjusts his control strategy. At b, the aircraft highly deviates from the glide path and it seems that the pilot has to take the aircraft back to the glide path immediately. Actually, at c, the aircraft is getting close to the glide path and the pilot turned back to the previous state B. At d, the aircraft is almost on the glide path, and the pilot switches to control state A. The elevator angle oscillation also decreases.

Fig. 4 PC-based flight simulator.

The SS model is assumed to be a PD controller. Table 2 shows the obtained model parameters (PD gains) at each state. In this simulation, a negative elevator angle indicates the pull-up direction. Note that the θ and ψ_t can be reformulated to θ_{rev} and $\psi_{t,\mathrm{rev}}$, as in the following expression:

$$\theta = [\theta_1 \quad \theta_2 \quad \theta_3 \quad \theta_4];$$

$$\psi_t = [\mathrm{Y}_{t=t-0.2} \quad \mathrm{dY/dt}_{t=t-0.2} \quad \mathrm{dY/dt}_{t=t-0.7} \quad 1.0];$$

$$\theta_{\mathrm{rev}} = [\theta_1 \quad \theta_2 + \theta_3 \quad -\theta_3 \Delta t \quad \theta_4];$$

$$\psi_{t,\mathrm{rev}} = [\mathrm{Y}_{t=t-0.2} \quad \mathrm{dY/dt}_{t=t-0.2} \quad (\mathrm{dY/dt}_{t=t-0.2} - \mathrm{dY/dt}_{t=t-0.7})/\Delta t \quad 1.0];$$

$$\Delta t = 0.7 - 0.2 = 0.5$$

The physical meaning of the elements of θ_{rev} are proportional (P) gain, derivative (D) gain, second-order D gain, and bias, respectively, where a positive gain indicates the stable direction. A second-order D gain is sometimes used for look ahead, but a negative gain indicates a delay of reaction.

In state A, which is the standard state according to the result, all gains are relatively low when compared with those of other states. This matches with the notion that, in the normal condition, where the aircraft is almost on the glide path, the pilot does not control the elevator aggressively. In state B, the D gain becomes high. It seems that the pilot tries to stabilize the pitch angle for which the change may be due to wind. In state C, the P gain is very high and the bias is very low. It means that the aircraft is far from the glide path, and the pilot tries to take the aircraft back to the glide path as soon as possible.

The states transition timing is considered in Fig. 6. Note that the reason why the pilot changes the state cannot be modeled in the SS model, but the timing of changing the states can be obtained. Therefore, the authors focus on the glide-path deviation and its rate. In this paper, the relationship between the timing of changing states and the glide-path deviation is considered. The vertical axis indicates the deviation from glide path, whereas the horizontal axis indicates its derivative. The three types of points for each state show the time histories for case 0-1. Recovering to a stable course on the glide slope will result in a counterclockwise spiral throughout the graph, ending at the origin. For example, the figure shows that the state transition b occurs when the aircraft is about -0.20 deg below the glide path and the derivative of glide slope deviation is about -0.03 deg /s. Thus, the conditions resulting in a state transition can be easily noticed from this graph. Based on the graph, the average relative position is lower than the glide path, which holds for most other cases as well. This result indicates that the pilot keeps the glide path slightly lower to not go above the glide path, and the state is changed if the aircraft is below a certain deviation. In the next chapter, the overall trend is also considered.

The time histories of throttle deflection also show an interesting trend. Except for the first decrease of throttle setting, the changes of throttle setting are observed following the change of state transition. This implies that the throttle control has a close relationship with elevator control, and the auto throttle system should be linked to the elevator control.

Table 2 SS-model parameters

	$\theta_{rev}1$ (P)	θ_{rev} 2 (D)	θ_{rev} 3 (D2)	θ_{rev} 4 (bias)
State A (standard state)	0.1736	−0.0011	−0.4386	−2.1239
State B (stabilizing state)	0.0003	1.8179	−0.7783	−2.7951
State C (path-fixing state)	0.8700	0.5402	−0.7071	−8.0685

Table 3 SS-model parameters in all cases

Case	State	$\theta_{rev}1$ (P)	$\theta_{rev}2$ (D)	$\theta_{rev}3$ (D2)	$\theta_{rev}4$ (bias)
0-1	Stabilizing	0.0003	1.8179	−0.7783	−2.7951
	Path fixing	0.8700	0.5402	−0.7071	−8.0685
	Standard	0.1736	−0.0011	−0.4386	−2.1239
0-2	Stabilizing	−1.3899	3.3770	−0.7607	1.6613
	Path fixing	0.6483	1.5108	−0.6288	−4.9247
	Standard	−0.0303	0.0798	−0.6232	−1.3203
0-3	Stabilizing	−0.3169	1.6026	−0.8009	−0.5199
	Standard	0.5363	−1.2567	−0.1847	−1.3740
	Path fixing	1.6092	−0.5092	−0.3033	−4.7433
	Stabilizing	−0.2289	0.7183	−0.5049	0.6160
10-1	Standard	0.0444	0.0785	−0.6156	−0.4193
	Path fixing	0.5942	−0.0692	−0.3609	−2.7839
10-2	Path fixing	0.5555	1.3041	−0.6806	−3.3703
	Standard	0.2219	−0.3990	−0.4907	−1.1936
10-3	Stabilizing	−0.8209	2.7504	−0.7282	−1.0173
	Path fixing	0.4180	2.0044	−0.5392	−2.1165
	Standard	0.0335	0.4051	0.5644	0.0596

According to these results, the pilot's intention is clearly observed at the state transitions. The data of the other cases is analyzed based on these findings in the next section.

B. Overall Analysis

All cases were processed like case 0-1 and the results are considered in this section. First, the gain parameters of each case are shown in Table 3. In all cases, except case 0-3, common characteristics are observed in the standard state: the P and D gains are relatively low. This implies that state A is a general control strategy for the pilot; the pilot does not control the elevator aggressively when the aircraft is almost on the glide path. A small turbulence is managed by the aircraft pitch stability. In case 0-3, the standard state has a different trend from the others but, as previously mentioned, the standard state is defined as the most likely observable state. Actually, in this case, the path deviation is oscillated during the flight, which makes this standard state similar to the path-fixing state.

In some states, a negative P gain is observed. However, in these states, a high positive D gain is simultaneously observed without exceptions. It is considered that the pilot tries to stabilize the aircraft under wind condition. As the pilot concentrates on stabilizing the aircraft, the P gain gets negative, as he cannot afford to pay attention on maintaining the target pitch angle. At the other states, the pilot tries to change the attitude and path angle in order to keep the glide path with a high P gain and a high or low bias. D2 gains are mostly negative, which means that the pilot response is slower than 0.2 s. However, according to the Bode diagram, the effect of D2 gains to phase margin is minor. In this paper, the effect of D2 gains is not discussed. It is also interesting to note that the headwind has no effects on the result, the fundamental control theory is independent on the considered wind conditions.

Next, the overall states transition timing is considered. In this paper, the threshold from some states to the path-fixing state is

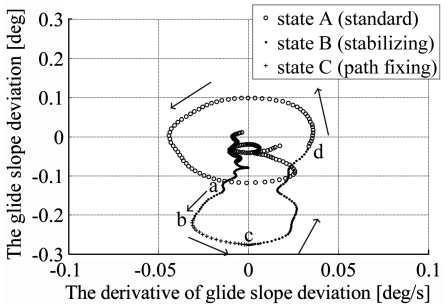

Fig. 6 The relationship between the deviation angle from glide path and its derivative (case 0-1).

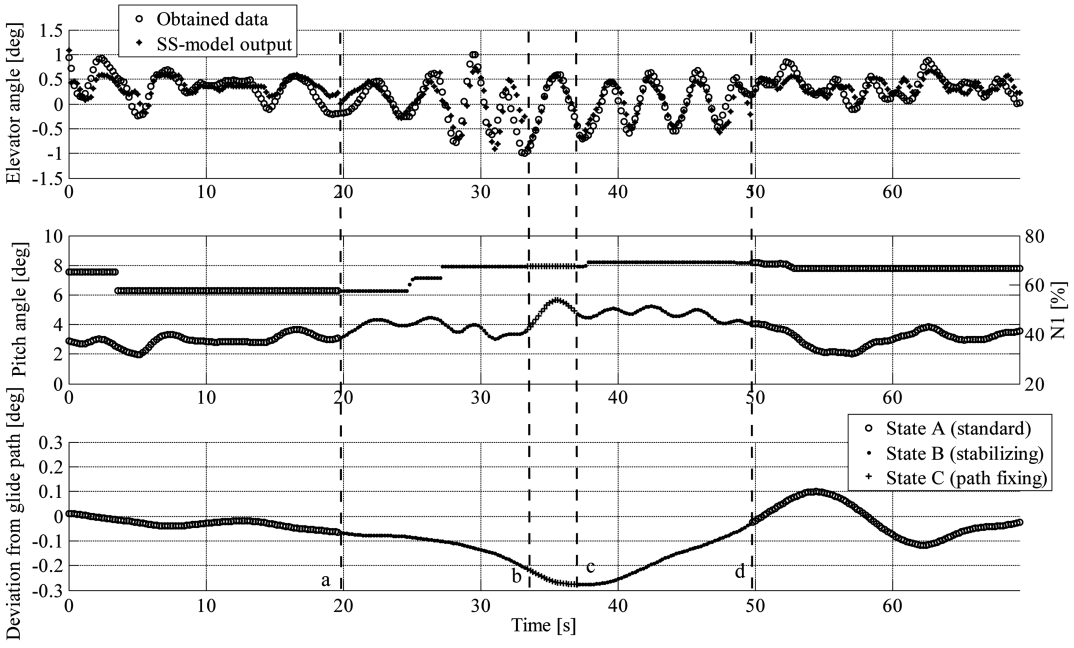

Fig. 5 Flight and control data (case 0-1).

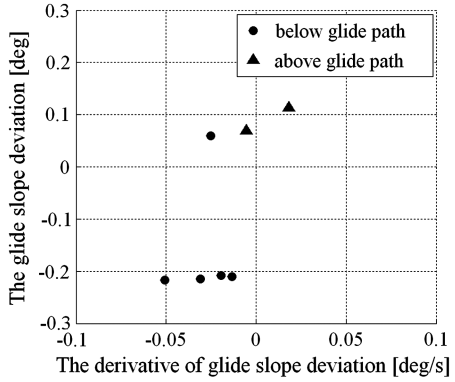

Fig. 7 The state transition timing.

discussed. When the state is switched to the path-fixing state, the pilot recognizes that the aircraft is deviating from the path and adjustment control is required. However, if the deviation is relatively small, the pilot will not alter the state. The threshold to path-fixing state is shown in Fig. 7. The graph format is the same as that of Fig. 6. The circles indicate state transitions to the path-fixing state when the aircraft is pulled up in path-fixing state, and the triangles transitions to a path-fixing state when the aircraft is pushed down in path-fixing state. In this figure, only the timing of the transitions to the path-fixing state is indicated. The figure clearly shows the thresholds for changing the state. When the aircraft deviated about -0.2 deg below or about 0.1 deg above the glide path, the pilot switched his control style to the path-fixing state. This result also indicates that the pilot does not alter the sensitivity to the glide-slope deviation when the state is switched to the path-fixing state. One point (case 10–3) is located above 0 deg of the glide-path deviation, though actually the aircraft is always between 0 and 0.2 deg of the glide-path deviation in this case. In this case, the airspeed is relatively higher than that in the other cases, and it seems that the pilot tries to decrease the airspeed by pitching the aircraft up. As a result, the aircraft is always deviated above the glide path. The parameters in Table 3 in this case are slightly different from those in the other cases: the D2 gain is positive in standard state and the D gain is relatively higher in the path-fixing state. However, in the rest of the cases, similar trends are observed. Although, as there are only two cases where the aircraft is above the glide path, no conclusive statements can be made, this result indicates that the state transition timing to path fixing is asymmetrical with respect to the position above or below the glide path. This is consistent with what we observed before for case 0-1. It also implies that deviation above the glide path is more critical than below it.

In this way, a pilot's control strategy and decision making during the final approach can be explained based on the SS model, as shown above.

V. Conclusions

In this paper, human pilot control of the approach was modeled using the SS model. The physical meaning can easily be understood from this model. The necessary inputs for this model were chosen, and the pilot models were constructed from data of simulated landings by a retired B747 pilot under different wind conditions. According to the results, three states to keep the glide path were recognized: a standard state, a stabilizing state, and a path-fixing state. In each case, common characteristics were observed. The timing of the state transition to path-fixing state was also considered, and an asymmetry was observed when the aircraft deviated above and below the glide path. The results clarified the pilot's control strategy and decision making. It is expected that this modeling method can be applied to construct an auto pilot system.

References

[1] "Human Factors in Fatal Aircraft Accidents," Bureau of Air Safety Investigation, Secretary of the Department of Transport and Regional Development, Civic Square, Australia, 1996.

[2] Suzuki, S., Sakamoto, Y., Sanematsu, Y., and Takahara, H., "Analysis of Human Pilot Control Inputs Using Neural Network," *Journal of Aircraft*, Vol. 43, No. 3, 2006, pp. 793–796. doi:10.2514/1.16898

[3] Mori, R., Suzuki, S., Sakamoto, Y., and Takahara, H., "Analysis of Visual Cues During Landing Phase by Using Neural Network Modeling," *Journal of Aircraft*, Vol. 44, No. 6, 2007, pp. 2006–2011. doi:10.2514/1.30208

[4] Arbib, M. A., *Brains, Machines and Mathematics*, 2nd ed., Springer–Verlag, New York, 1987.

[5] Iiguni, Y., Akiyoshi, H., and Adachi, N., "An Intelligent Landing System Based on a Human Skill Model," *IEEE Transactions on Aerospace and Electronic Systems*, Vol. 34, No. 3, 1998, pp. 877–882. doi:10.1109/7.705894

[6] Sekizawa, S., Inagaki, S., Suzuki, T., Hayakawa, S., Tsuchida, N., Tsuda, T., and Fujinami, H., "Modeling and Recognition of Driving Behavior Based on Stochastic Switched ARX Model," *IEEE Transactions on Intelligent Transportation Systems*, Vol. 8, No. 4, 2007, pp. 593–606. doi:10.1109/TITS.2007.903441

[7] Rabiner, L. R., "A Tutorial on Hidden Markov Models and Selected Applications in Speech Recognition," *Proceedings of the IEEE*, Vol. 77, No. 2, 1989, pp. 257–286. doi:10.1109/5.18626

[8] Mori, R., Suzuki, S., and Takahara, H., "Optimization of Neural Network Modeling for Human Landing Control Analysis," AIAA Infotech at Aerospace 2007 Conference and Exhibit, AIAA, Paper 2007-2840, Washington, D.C., 2007.